

Host Cell Traversal Is Important for Progression of the Malaria Parasite through the Dermis to the Liver

Rogerio Amino,^{1,2,6} Donatella Giovannini,^{1,6} Sabine Thiberge,¹ Pascale Gueirard,¹ Bertrand Boisson,¹ Jean-François Dubremetz,³ Marie-Christine Prévost,⁴ Tomoko Ishino,^{1,5} Masao Yuda,⁵ and Robert Ménard^{1,*}

¹Unité de Biologie et Génétique du Paludisme, Institut Pasteur, 28 Rue du Dr Roux, 75724 Paris cedex 15, France

²Departamento de Bioquímica, Universidade Federal de Sao Paulo, Rua Três de Maio 100, 04044-020, Sao Paulo, Brazil

³UMR 5539 CNRS, Université de Montpellier 2, Place Eugène Bataillon, 34095 Montpellier cedex 05, France

⁴Plate-forme de microscopie électronique, Institut Pasteur, 25-28 rue du Dr Roux, 75724 Paris cedex 15, France

⁵Mie University, School of Medicine, 2-174 Eodobashi, Tsu, Mie 514-0001, Japan

⁶These authors contributed equally to this work.

*Correspondence: rmenard@pasteur.fr

DOI 10.1016/j.chom.2007.12.007

SUMMARY

The malaria sporozoite, the parasite stage transmitted by the mosquito, is delivered into the dermis and differentiates in the liver. Motile sporozoites can invade host cells by disrupting their plasma membrane and migrating through them (termed cell traversal), or by forming a parasite-cell junction and settling inside an intracellular vacuole (termed cell infection). Traversal of liver cells, observed for sporozoites in vivo, is thought to activate the sporozoite for infection of a final hepatocyte. Here, using *Plasmodium berghei*, we show that cell traversal is important in the host dermis for preventing sporozoite destruction by phagocytes and arrest by nonphagocytic cells. We also show that cell infection is a pathway that is masked, rather than activated, by cell traversal. We propose that the cell traversal activity of the sporozoite must be turned on for progression to the liver parenchyma, where it must be switched off for infection of a final hepatocyte.

INTRODUCTION

Malaria infection is initiated when an *Anopheles* mosquito injects *Plasmodium* sporozoites into the dermis of the host (Sidjanski and Vanderberg, 1997; Matsuoka et al., 2002; Vanderberg and Frevert, 2004; Amino et al., 2006; Yamauchi et al., 2007). Sporozoites travel from the site of mosquito bite to the liver, where they enter and settle inside hepatocytes. They then multiply and differentiate into the parasite form called merozoite, which infects red blood cells and causes the symptoms of the disease.

The journey and fate of the sporozoite in the mammalian host is still a poorly documented part of the parasite life cycle. A recent quantitative in vivo imaging study has revealed that sporozoites inoculated by a mosquito reach not only the liver, via the bloodstream, but also the lymph node draining the site of the mosquito bite, where most are internalized inside dendritic cells

and some can initiate development (Amino et al., 2006). In liver sinusoids, sporozoites interact with resident macrophages, the Kupffer cells, which are thought to act as necessary gates to the underlying parenchyma (Pradel and Frevert, 2001; Frevert et al., 2005; Baer et al., 2007).

The elongated sporozoite cell displays an active gliding locomotion on solid substrates in vitro and in host tissues, reaching speeds up to 4 $\mu\text{m/s}$, which is powered by a submembranous actin-myosin motor (Ménard, 2001; Kappe et al., 2004). Using this motor, the sporozoite can invade host cells in two distinct ways. Like other invasive stages of Apicomplexa protozoa, it can penetrate the cell inside a so-called parasitophorous vacuole (PV) formed by invagination of the host cell plasma membrane. Typically, the apicomplexan zoite forms an intimate junction between its anterior pole and the contacting host cell surface, the so-called moving junction (MJ), on which it must exert force to pull itself inside the nascent vacuole (Hollingdale et al., 1981; Sibley, 2004). This process, termed here cell infection, is a prerequisite for complete sporozoite differentiation into merozoites and occurs in vivo inside hepatocytes.

The sporozoite can also disrupt host membranes and migrate through and out of the cell. The cell traversal behavior of the sporozoite was first described with macrophages (Vanderberg et al., 1990) and later shown to also occur with epithelial cells and fibroblasts (Mota et al., 2001). In the *P. berghei* species that infect rodents, this activity was documented in vivo only in the liver (Frevert et al., 2005; Mota et al., 2001). Based on work performed with *P. berghei*-hepatocyte in vitro systems, the current view is that, in vivo, sporozoites traverse several hepatocytes before infecting a final hepatocyte, and that the former step has a dual activating role on the latter. First, it appeared to render the sporozoite competent for infecting a final cell inside a PV, by inducing progressive exocytosis of the parasite proteins specifically involved in this process (Mota et al., 2002). Second, it was found to cause the release of hepatocyte growth factor (HGF) from traversed cells, and HGF to promote parasite development in infected cells via cMET-dependent signaling pathways (Carrolo et al., 2003).

More recent work, however, has challenged these conclusions. Inactivation in *P. berghei* of the genes named *spect* (Ishino

et al., 2004) or *spect2* (Ishino et al., 2005a) impaired the sporozoite capacity to traverse hepatoma cells lines without affecting its ability to develop inside these cells. Host cell traversal was found to be important for sporozoite crossing the liver sinusoid barrier, possibly by migrating through Kupffer cells (Ishino et al., 2004, 2005a). SPECT and SPECT2 are structurally unrelated secretory proteins, and SPECT2 possesses a typical membrane-attack/perforin (MACPF)-like domain, found in pore-forming proteins such as components of the mammalian complement system and perforin.

Here, to further study the role of host cell traversal in vivo, we rendered *spect(-)* and *spect2(-)* sporozoites fluorescent and characterized their behavior by real-time imaging both in vivo and in vitro.

RESULTS

Generation and Cell Traversal Activity of the ConF, SpectF, and Spect2F Sporozoites

We first generated a fluorescent *P. berghei* ANKA clone, named ConF, by integrating at the *DHFR-TS* locus of the wild-type the *GFP* gene fused to *HSP70* regulatory sequences (see Figure S1 available online). Erythrocytic stages of the *P. berghei spect(-)* and *spect2(-)* clones (Ishino et al., 2004, 2005a) were separately mixed with erythrocytic stages of the ConF clone and transmitted to *Anopheles stephensi* mosquitoes, where meiosis and random chromosome segregation occur. The double transgenic parasites *spect-1/gfp+* and *spect2-1/gfp+* emerging from cross-fertilized zygotes, named SpectF and Spect2F, respectively, were cloned as erythrocytic stages after parasite cycling (Figure S1).

The ConF, SpectF, and Spect2F clones were then transmitted to *Anopheles stephensi* mosquitoes, and 18 days after parasite transmission, similar numbers of sporozoites in the three clones were present in the mosquito salivary glands. In matrigel, ~80% of the sporozoites in the three clones glided with an average velocity of ~1.4 $\mu\text{m/s}$ for up to 30 min at 37°C (Figure 1A and Figure S2), typically following a corkscrew path while occasionally moving randomly. To examine sporozoite capacity to wound host cell plasma membranes, sporozoites were recorded for 30 min inside matrigels containing host cells in the presence of SYTOX Orange, a nucleic acid stain that penetrates cells with compromised plasma membranes and fluoresces in the nucleus. Cells fluorescent after 30 min were individually examined and scored as wounding events when cell fluorescence started less than 2 min after sporozoite contact. ConF sporozoites wounded all cell types tested, i.e., mast cells and dermal fibroblasts (data not shown), primary hepatocytes (Figure 1B), and HepG2 hepatoma cells (Figure 1C and Movie S1). In primary hepatocytes, ConF sporozoites (multiplicity of infection = 1) provoked an average of 1.8 wounding events/sporozoite/hr. In contrast, SpectF and Spect2F sporozoites did not induce host cell fluorescence in any of the cell types tested. The *spect* and *spect2* genes are thus both dispensable for sporozoite gliding in three-dimensional (3D) matrices but individually critical for the membrane-damaging capacity of the sporozoite.

Host Cell Traversal Is Important in the Dermis of the Host

To test whether the traversal activity was important during the skin phase of the sporozoite's journey, we compared infectivity

of intravenously or subcutaneously injected wild-type or *spect(-)* sporozoites in animals treated with liposome-encapsulated clodronate. Clodronate destroys macrophages in the liver and, to a lesser extent, in the spleen, but not in other tissues (van Rooijen et al., 1997). In these animals, intravenously injected wild-type and mutant sporozoites had similar infectivity, whereas subcutaneously injected mutant sporozoites were ~5- to 10-fold less infective than the wild-type (Figure 2A). This suggested that the traversal activity was important during the sporozoite transit in the skin.

We then examined by intravital imaging the fate of sporozoites in the dermis of mice after natural transmission. A single mosquito was allowed to probe the ear of an anesthetized Hairless mouse for 1 min, and the probed site was observed by spinning disk confocal microscopy (Amino et al., 2007) at various times postinfection (p.i.). Like *P. berghei* NK65 sporozoites (Amino et al., 2006), most (~80%) ANKA ConF sporozoites glided at an average speed of ~1–2 $\mu\text{m/s}$, following a tortuous path (Figures 2B and 2C; Figure S3). In contrast, most mutant sporozoites were immotile, with only ~10% of the sporozoites in the two mutant clones gliding between 15 and 30 min p.i. (Figures 2B and 2C; Figure S3). In agreement with their normal gliding in 3D matrices, the path and speed of the few mutant sporozoites that were motile were similar to those of ConF sporozoites. Therefore, most of the mutants, despite normally gliding in 3D matrices, were rapidly immobilized in the dermis, presumably by host cells they cannot traverse.

Host Cell Traversal Is Important for Resisting Clearance by Phagocytes in the Dermis

We next tested whether host leukocytes were involved in the arrest of cell traversal-deficient mutants in the dermis. Spect2F sporozoites were transmitted to Hairless mice by mosquito bite, and the site of bite was extracted, stained with antibodies to CD11b, a leukocyte-specific antigen, and examined by confocal microscopy. At 5 and 30 min p.i., when ~75% of the control sporozoites are motile, about 10% and 50% of the mutant sporozoites, respectively, were associated with CD11b+ cells (Figure 3A), and ~25% of the mutants could be detected inside these cells after 30 min (Figure 3B). Similar results were obtained using SpectF sporozoites (data not shown).

Interactions between SpectF sporozoites and host phagocytes were then imaged in real-time in *lys-gfp* mice (Faust et al., 2000), in which myelomonocytic cells (macrophages, neutrophil granulocytes, and dendritic leukocytes) express GFP (Figures 3C and 3D). At the mosquito bite sites, weakly fluorescent, resident phagocytes were present, while brightly fluorescent cells were recruited starting at ~25 min p.i. (Figure 3C). Mutant sporozoites were rapidly immobilized, as early as 3 min p.i., and were frequently seen in contact with dermal cells, labeled by red fluorescent BSA, or green fluorescent phagocytic cells. The fluorescence of many mutant sporozoites gradually faded during 1 hr observation periods (Figure 3D, blue inset). Importantly, however, although cell traversal-deficient sporozoites could be destroyed by phagocytic cells, the fluorescence of some sporozoites remained unchanged with time (Figure 3D, red inset), suggesting that immobilized mutants could also escape degradation.

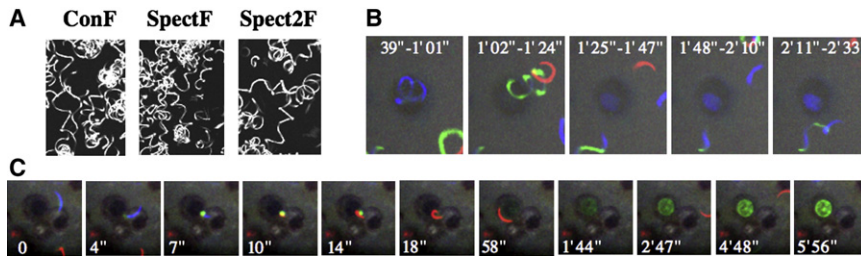


Figure 1. Sporozoite Gliding Motility and Cell Traversal Ability

(A) Sporozoite motility in matrigel. Sporozoites were mixed with matrigel and were imaged in multiple z layers for 5 min. The path of sporozoites is represented by the maximum intensity projection of the fluorescent signal.

(B and C) Time-lapse microscopy of a ConF sporozoite traversing a primary hepatocyte (B) or a HepG2 hepatoma cell (C) in the presence of SYTOX Orange. Sequential images are shown as maximum intensity projections of the fluorescence

signal recorded during the time intervals (B) or time points (C) indicated. Each Z plane, acquired using the 488 nm (GFP) and the 568 nm (SYTOX) channels, was projected over time and pseudocolored: Z4 (depth of 40 μ m) in red, Z5 (depth of 50 μ m) in green, and Z6 (depth of 60 μ m) in blue.

Cell Traversal-Deficient Sporozoites Are Arrested by and Readily Invade Dermal Fibroblasts

The fact that a proportion of mutant sporozoites immobilized in the dermis were not associated with CD11b+ cells and were not destroyed by phagocytes suggested that mutants might also invade nonprofessional phagocytes. To test this, we examined sporozoite interactions with fibroblasts, a major nonphagocytic cell type in the dermis. ConF, SpectF, or Spect2F sporozoites were mixed with either human foreskin fibroblasts (HFF) or mouse dermal fibroblasts (ATCC CRL-2017) in matrigel, the trajectories of gliding sporozoites were visualized as maximal intensity projections, and the proportion of immotile sporozoites was counted at various times (Figures 4A–4D). For up to 30 min, ~80% of the ConF sporozoites moved in a pattern indistinguishable from that in cell-free matrigel, showing that the pres-

ence of host cells did not affect motility of normal sporozoites. In contrast, less than 20% of the sporozoites in both mutant clones were still motile after 30 min (Figures 4C and 4D), most mutant sporozoites being immobilized in association with a cell (Figure 4B). Time-lapse imaging showed that mutant sporozoites were suddenly arrested upon the first contact with a fibroblast, frequently remaining bound to the host cell surface for extended periods of time (Figure 4E and Movie S2). To test whether mutant sporozoites could penetrate fibroblasts, SpectF sporozoites were incubated with HFF cells, and after 30 min thin sections were examined by transmission electron microscopy (TEM). SpectF sporozoites were detected inside cells and surrounded by a membrane (Figure 4F), showing that mutant sporozoites could also be arrested by and invade dermal fibroblasts.

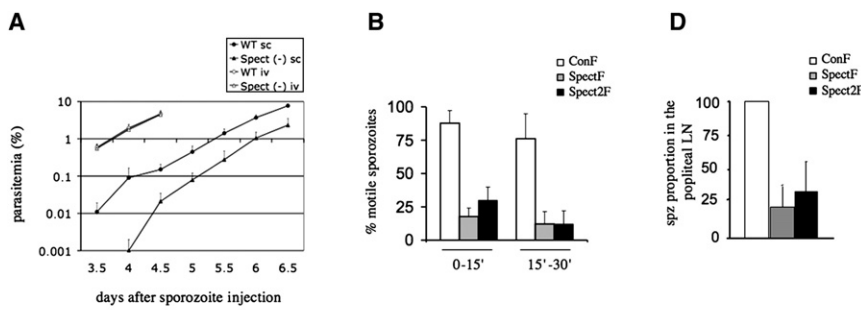
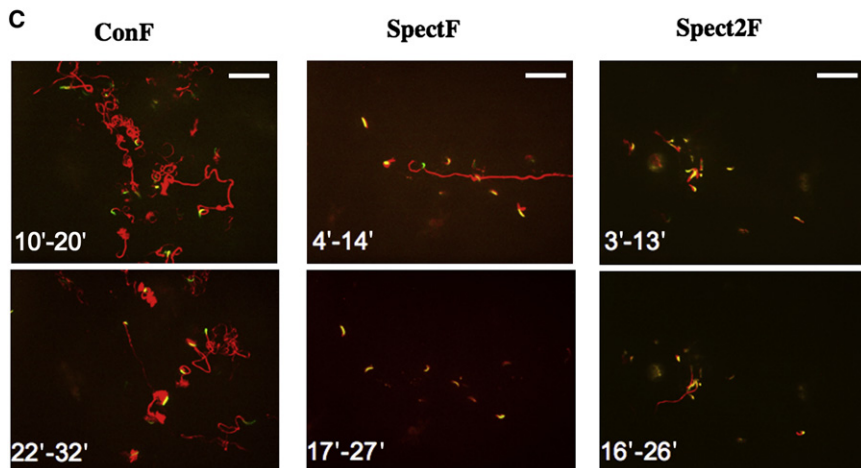


Figure 2. Host Cell Traversal Is Important in the Skin

(A) Infectivity of wild-type and *spect(-)* sporozoites injected intravenously (iv; 30,000) or subcutaneously (sc; 50,000) in clodronate treated rats (n > 5 animals). The graph shows the average + SD of the parasitemia in logarithmic scale.

(B and C) Motility of sporozoites injected by a mosquito into the ear of a Hairless mouse. (B) Percentage of motile parasites during the first 15 min and between 15 and 30 min after the bite. The bar represents the average + SD in 10 min of analysis (n = 3–6 bites). Numbers of sporozoites analyzed: ConF = 174, SpectF = 157, Spect2F = 195. (C) Maximum intensity projections of the fluorescent signal (in red) of sporozoites gliding during the indicated period of time. Scale bar, 50 μ m.

(D) Proportion of cell traversal-deficient mutants that reach the popliteal lymph node (LN) 2 hr after infection compared to the wild-type (n = 5 animals). The bars represent the average + SD of five experiments for each mutant.



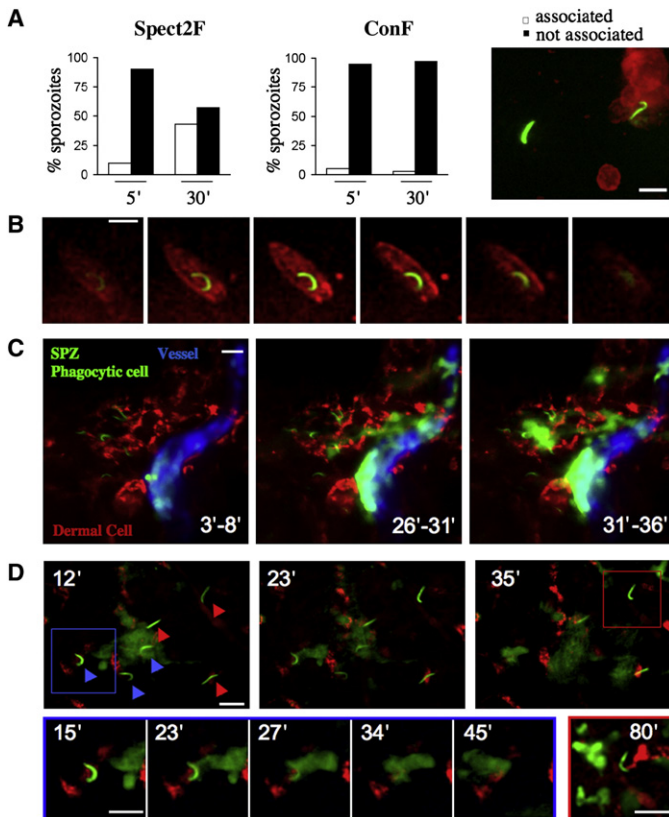


Figure 3. Mutant Sporozoite Interactions with Host Leukocytes

(A and B) Spect2F and ConF interaction with CD11b⁺ cells in Hairless mice. A mouse was bitten by Spect2F- or ConF- infected mosquitoes in the abdomen, and the bite site was extracted, fixed with 4% paraformaldehyde/PBS, stained with rat anti-mouse CD11b-Alexa 647 mAb, and analyzed by confocal microscopy. Scale bars, 15 μ m. (A) Percentage of Spect2F or ConF sporozoites associated or not with CD11b⁺ cells 5 and 30 min after the bite (86 Spect2F and 49 ConF sporozoites analyzed). Similar results were obtained using SpectF sporozoites ($n = 51$). (B) A SpectF sporozoite inside a CD11b⁺ cell in the dermis. The panel shows 6 z stacks (z step, 1 μ m) recorded sequentially with a double wavelength excitation of 488 nm (GFP) and 647 nm (CD11b). The centrality of the sporozoite within the panel of z stacks confirms its intracellular localization. (C and D) Fate of SpectF sporozoites in the dermis of *lys-gfp* mice.

(C) Time-lapse microscopy of leukocyte recruitment at the sporozoite-containing site in the dermis. Dermal cells, which take up red-fluorescent BSA injected intravenously into the animal prior to imaging, are labeled in red, and the blood vessel is represented in blue. A massive recruitment of brightly fluorescent cells is seen starting at ~ 25 min p.i. that progressively infiltrate the sporozoite-containing site. Scale bar, 30 μ m.

(D) Time-lapse microscopy of the fate of six dermal SpectF sporozoites. The upper panel (three images) follows the six sporozoites over time: three (indicated by blue arrowheads) no longer fluoresce after 35 min, while three others (indicated by red arrowheads) still fluoresce after that time. The lower left time-lapse view (five images) shows the progressive degradation of the leftmost sporozoite of the upper panel (blue-squared). The lower right image shows the red-squared sporozoite of the upper panel that still fluoresces after 80 min. Scale bars, 15 μ m.

Host Cell Traversal Is Not Essential for Crossing Endothelial Barriers in the Dermis

Next, we tested whether host cell traversal played a role during sporozoite crossing endothelial barriers in the dermis. We have shown that sporozoites can actively cross the walls of both blood and lymphatic vessels in the dermis, and that $\sim 1\%$ of the *P. berghei* NK65 sporozoites inoculated in the mouse footpad by subcutaneous injection terminate their journey and accumulate in the first draining (popliteal) lymph node (Amino et al., 2006). Similarly, after injection of 10^4 ConF sporozoites in the footpad of mice, an average of $\sim 1\%$ – 2% was counted in the popliteal node after 2 hr. To compare the capacity of mutant and control sporozoites to reach the popliteal node, we injected the same number of SpectF or Spect2F sporozoites in the footpad of a mouse and of ConF sporozoites contralaterally and counted the number of sporozoites in the popliteal nodes 2 hr p.i. (Figure 2D). The numbers of SpectF and Spect2F sporozoites were only 25% and 32% of that of ConF sporozoites, respectively. The similar decrease in the proportion of mutant sporozoites in the lymph node at 2 hr p.i. (Figure 2D) and in the proportion that initially glided in the dermis (Figure 2B) thus suggests that mutant sporozoites have no specific defect in crossing the wall of lymph vessels. The residual infectivity of mutant sporozoites delivered to normal rats by mosquito bite (data not shown) or injected subcutaneously in normal (data not shown) or clodronate-treated animals (Figure 2A) also indicates that cell traversal is not essential for crossing the wall of dermal blood vessels. Therefore, immobilization of mutant sporozoites inside leukocytes or other cell types in the dermis seems to constitute a primary

defect, rather than a consequence of an inability to cross endothelial barriers in the dermis.

Cell Traversal Retards, Rather Than Activates, Hepatocyte Infection

We next investigated sporozoite traversal of hepatocytes. Previous studies have suggested that sporozoites traverse several hepatocytes in vivo before final infection (Fever et al., 2005; Mota et al., 2001). In agreement with this, ConF sporozoites were found to glide extensively in the liver parenchyma before finally arresting, as exemplified in Figure S4 (Movie S4). To study cell traversal in the liver parenchyma, we first compared the differentiation of ConF, SpectF, and Spect2F sporozoites in rodent primary hepatocytes. *P. berghei* sporozoites develop into exoerythrocytic forms (EEF) that yield after ~ 60 hr thousands of mature merozoites, the erythrocyte-infecting stage (Sturm et al., 2006). No difference was noticed between the three clones in the number, size, and fluorescence intensity of EEF at 4, 12, 24, or 48 hr in rat (Figure 5A) or mouse (data not shown) primary hepatocytes. The three clones generated merozoites with similar infectivity to rats, as measured by prepatent periods of infection (data not shown). Therefore parasite development inside hepatocytes does not appear to depend on prior traversal of these cells.

To examine sporozoite entry into primary hepatocytes, infection events (parasites internalized inside a vacuole) were measured after 1 hr incubation, when sporozoites are no longer motile and invasive. For this, samples fixed at 1 hr were labeled with antibodies to the sporozoite CS surface protein to discriminate extracellular (red) from intracellular (green) parasites, and infection

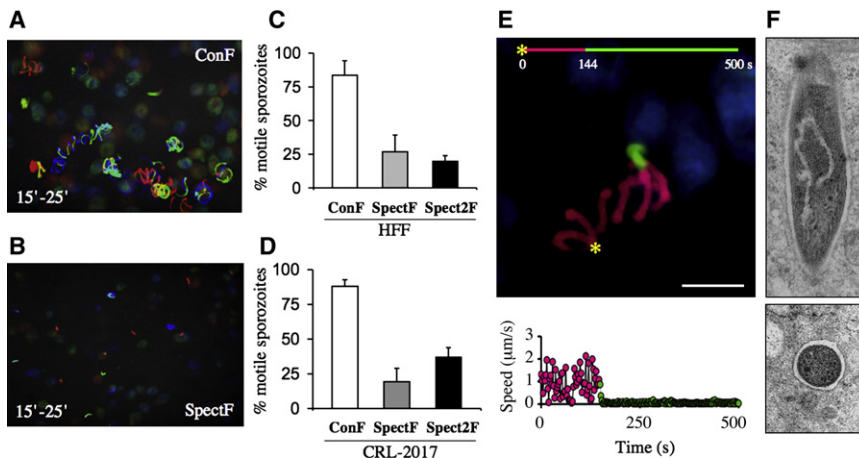


Figure 4. Mutant Sporozoite Interaction with and Invasion of Dermal Fibroblasts In Vitro

(A–D) Sporozoites were mixed with matrigel containing fibroblasts and motility recorded by videomicroscopy. (A and B) Maximum intensity projections of ConF (A) and SpectF (B) sporozoites in HFF-containing matrigel recorded between 15 and 25 min incubation. (C and D) Percentage of motile sporozoites after 10 min incubation in HFF- or CRL-2017-containing matrigel. The bar represents the average \pm SD in 10 min of analysis ($n = 3$ –6 samples). Numbers of sporozoites analyzed using HFF cells: ConF = 110, SpectF = 40, Spect2F = 99; using CRL-2017 cells: ConF = 171, SpectF = 86, Spect2F = 175.

(E) Immobilization of a representative SpectF sporozoite upon contact with a HFF cell. Upper panel: maximum intensity projection of the parasite (in red before the initial contact, green after). The timing of the color code is indicated in seconds. Lower panel: velocity profile of the sporozoite.

(F) TEM pictures of SpectF sporozoites internalized in HFF cells after 30 min incubation.

events counted as green parasites (see [Experimental Procedures](#)). After 1 hr incubation with primary hepatocytes, $\sim 20\%$ of the initial sporozoites in the three clones were scored as infection events (Figure 5B). Similar results were obtained using CRL-2017 dermal fibroblasts (Figure 5B). The kinetics of cell invasion by mutant and control sporozoites were then compared by TEM analysis of primary hepatocytes fixed after 10 or 30 min incubation. Using Spect2F sporozoites, at both 10 and 30 min a high proportion of cells (37%) contained an intracellular parasite, and as expected, 100% of the intracellular Spect2F sporozoites were surrounded by a membrane (Figure 5C and Figure S5). Instead, using ConF sporozoites, a lower proportion of cells ($\sim 15\%$) contained an intracellular parasite, and the proportion of intracellular parasites surrounded by a membrane increased from 35% to 60% after 10 and 30 min, respectively (Figure 5C and Figure S5).

The rapid kinetics of hepatocyte invasion by mutant sporozoites was confirmed by CS staining assays (Figures 6A and 6B). Using Spect2F, the first intracellular sporozoites were detected after only 2 min incubation, $>2\%$ of the sporozoites appeared bicolor (half red/CS-half green/GFP) during the first 4 min, presumably fixed during cell penetration, and the final levels of 20% of internalized sporozoites were reached after only 10 min. Similar results were obtained during entry of Spect2F sporozoites into dermal fibroblasts (Figure S6) and with SpectF sporozoites in both cell types (data not shown). Time-lapse imaging of Spect2F sporozoites incubated with primary hepatocytes readily showed sporozoites displaying and moving through a constriction, suggestive of a MJ, at the site of host cell contact (Figure 6C and Movie S3). Finally, TEM analysis of samples fixed at 3 min detected Spect2F sporozoites entering primary hepatocytes while forming a MJ with the host cell surface (Figure 6D), which is seen here for the first time between a *Plasmodium* sporozoite and a mammalian cell.

Constitutive Infection by Mutant Sporozoites Is Due to Lack of Cell Traversal

Finally, we addressed the possibility that the “rapid invader” phenotype of the mutants might be due to secondary changes

on their surfaces, conferring gain-of-function infective capacities that would normally be activated by traversal of host cells. We first compared adhesion of control and mutant sporozoites to confluent CRL-2017 monolayers in the presence of $1 \mu\text{g/ml}$ cytochalasin (Figures 7A and 7B), which prevents parasite internalization into but not attachment to host cells, or using sporozoites metabolically inhibited by 0.03% azide (data not shown). No significant difference between adhesion of control and mutant sporozoites to cells was noticed in any of these conditions. Also, using real-time qPCR, we compared in salivary gland sporozoites the levels of transcripts encoding the 13 parasite products currently known or suspected to be involved in sporozoite adhesion and/or invasion of host cells, listed in Figure 7C. No significant difference was observed in expression of any of these genes in ConF, SpectF, and Spect2F sporozoites (Figure 7C). These data confirm the view that the “rapid invader” phenotype of the mutants is a direct consequence of their lack of cell traversal.

DISCUSSION

The primary function of the host cell traversal capacity of the *Plasmodium* sporozoite, first described by Vanderberg and collaborators in 1990, remains controversial. Because the traversal activity in vivo was documented first in hepatocytes in rodents, it was presumed that traversing hepatocytes was an important step that would directly favor the final infection step in a PV (Mota et al., 2001). In vitro data have suggested that traversal of hepatocytes was essential in two distinct ways: by rendering the sporozoite competent for entering a cell inside a PV (Mota et al., 2002) and by modifying the infected hepatocyte for optimal development of the parasite in the PV (Carrolo et al., 2003). The results presented here, along with previous studies (Ishino et al., 2004, 2005a), suggest a different contribution of the cell traversal activity.

We show here that this activity is first important in the dermis of the host, where it primarily prevents sporozoite destruction by phagocytic cells. A secondary effect of cell traversal might be to avoid infection of cells that sporozoites can penetrate inside

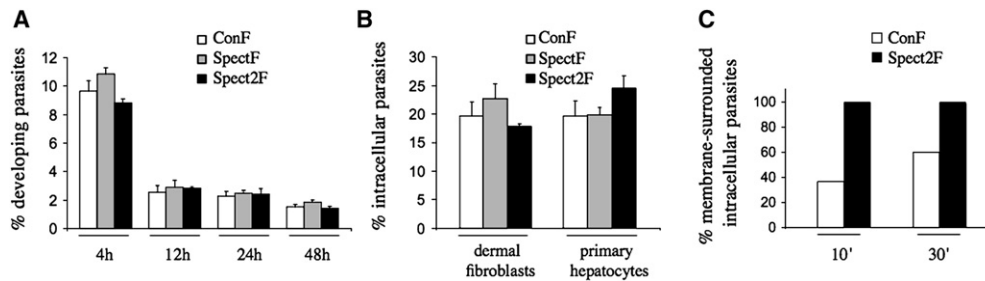


Figure 5. The Cell Traversal-Deficient Mutants Infect Primary Hepatocytes at Normal Levels and Normally Develop inside These Cells

(A) Percentage of parasites developing inside rat primary hepatocytes. Salivary gland sporozoites (15×10^4) were added to nonconfluent cells (multiplicity of infection = 1), and maturing parasites were counted in the entire well by fluorescence microscopy after various incubation times at 37°C . (B) Percentage of sporozoites internalized in CRL-2017 dermal fibroblasts and rat primary hepatocytes after 1 hr incubation. Infections were initiated as in (A), samples were labeled with anti-CS antibody after 1 hr, and the proportion of intracellular parasites counted by fluorescence microscopy as green parasites. The bars in (A) and (B) represent the average + SD of three independent experiments each performed in triplicate. (C) Percentage of intracellular parasites surrounded by a vacuolar membrane in rat primary hepatocytes. Infections were processed for TEM after 10 or 30 min incubation, and 159 ConF (in 620 cells) and 111 Spect2F (in 269 cells) intracellular parasites were counted.

a vacuole but are not their final destination, such as dermal fibroblasts. These two roles might serve the sporozoite at other steps of its journey to the liver parenchyma, including, as previously suggested, for resistance to clearance by Kupffer cells in liver sinusoids (Ishino et al., 2004, 2005a). We found no evidence, however, that cell traversal is important for crossing endothelial barriers in the dermis, and whether it is required for crossing the endothelium of liver sinusoids is still debated. Clodronate, which kills Kupffer cells, restores infectivity of the intravenously injected mutant sporozoites. This would suggest a role of cell traversal in resisting killing by Kupffer cells, but clodronate treatment might also create gaps in the liver sinusoidal barrier and thus artificial gates to the parenchyma (Baer et al., 2007). Therefore, cell traversal appears to be important in at least two steps of the sporozoite's journey: in the dermis, for freely moving until endothelial barriers are reached and for resisting attacks by phagocytic cells in the process, and in the liver sinusoids, presumably for resisting destruction by Kupffer cells.

The interactions between the cell traversal-deficient mutants and primary hepatocytes described here are irreconcilable with the currently accepted model of the role played by hepatocyte traversal in the sporozoite's life (Mota and Rodriguez, 2004; Leir-

iao et al., 2004; Waters et al., 2005; Prudencio et al., 2006). First, the normal differentiation of cell traversal-deficient parasites inside hepatocytes, as well as *in vivo* in the absence of Kupffer cells (Ishino et al., 2004, 2005a), demonstrates that parasite development does not depend on any factor released by wounded cells acting on infected cells. Second, the kinetics of cell infection by sporozoites, observed using both primary hepatocytes and dermal fibroblasts, clearly suggests that prior cell traversal retards, rather than activates, the final cell infection step. We found that mutant and control sporozoites only differed by the lack of cell traversal and a rapid/synchronized cell infection in the former, suggesting that lack of cell traversal directly causes (and might be sufficient for) the rapid invader phenotype. Therefore, the cell infection pathway unmasked by the lack of cell traversal in the mutants should also be constitutively available in the normal sporozoite. Successful cell infection by the normal sporozoite might only necessitate turning off the antagonistic cell traversal activity.

In this view, sporozoite entry inside a PV would require formation of the MJ and the PV as well as silencing of the cell traversal activity. The MJ and PV biogenesis, which clearly do not depend on prior cell traversal, might be triggered by host cell contact.

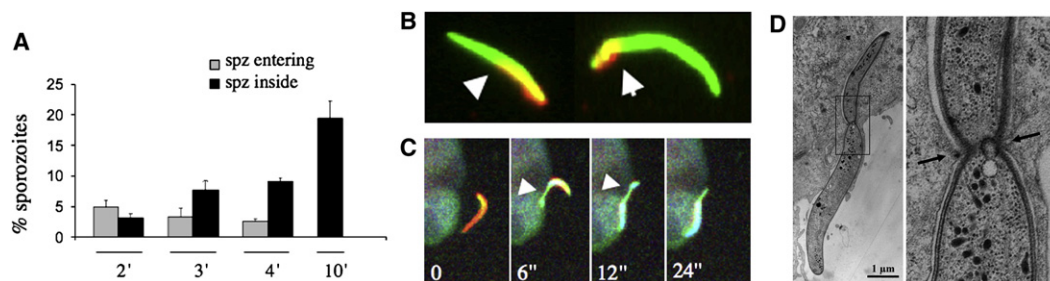


Figure 6. The Cell Traversal-Deficient Mutants Rapidly Invade Host Cells by Forming a Moving Junction

(A) Percentage of Spect2F sporozoites entering or fully internalized in rat primary hepatocytes during the first 10 min incubation. Infections were initiated as in Figure 5A, samples were labeled with anti-CS antibody after the various incubation times, and entering and intracellular sporozoites were scored as bicolor and green parasites, respectively. The bars represent the average + SD of three independent experiments each performed in triplicate.

(B) Representative merged pictures of entering, bicolor Spect2F sporozoites. The arrowheads indicate the junction between the extracellular (yellow) and intracellular (green) portions of the parasites.

(C) Time-lapse microscopy of a Spect2F sporozoite interacting with a primary hepatocyte in matrigel. Arrowheads point to the parasite constriction at the site of host cell contact. The time (in seconds) is indicated.

(D) TEM pictures of a Spect2F sporozoite entering a rat primary hepatocyte and zoom-in (right panel) on the host-parasite moving junction.

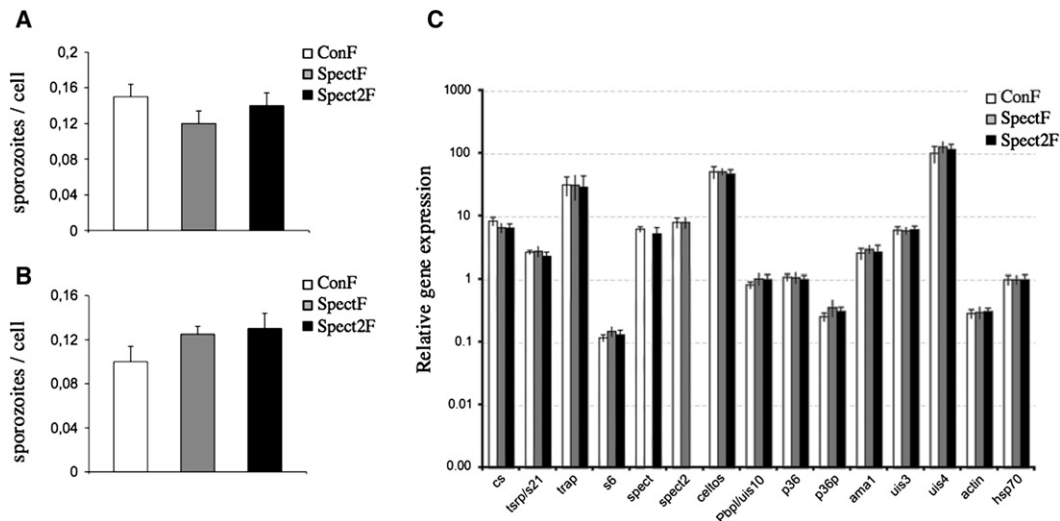


Figure 7. The Cell Traversal-Deficient Mutants Normally Adhere to Host Cells and Express Normal Levels of Adhesion/Invasion-Related Transcripts

(A and B) Confluent monolayers of murine CRL-2017 fibroblasts were incubated with 1.5×10^4 salivary gland sporozoites in the presence of 1 μ g/ml cytochalasin D, samples were not centrifuged (A) or centrifuged for 1 min at 4°C at 800 rpm to facilitate parasite-host cell interactions (B), and after 15 min incubation at 37°C the numbers of attached sporozoites per cell were counted. The bars represent the average + SD of triplicates.

(C) Histogram representation of qPCR analysis of gene expression in ConF, SpectF, and Spect2F sporozoites collected from salivary glands of mosquitoes at day 21 of infection. The genes tested are CS (Sinnis et al., 1994), TRSP (Labaied et al., 2007), TRAP (Sultan et al., 1997), S6 (Kaiser et al., 2004), spect (Ishino et al., 2004), spect2 (Ishino et al., 2005a), CeTOS (Kariu et al., 2006), Pbp/uis10 (Bhanot et al., 2005), P36 and P36p (Ishino et al., 2005b; van Dijk et al., 2005), AMA1 (Silvie et al., 2004), and UIS3 and UIS4 (Mueller et al., 2005a, 2005b). Mean values were obtained from three independent batches of sporozoites of each clone. x axis: genes tested; y axis: log scale of mean normalized expression (hsp70). Standard deviations for all genes tested were 20%–30% of gene expression, except for TRAP using Spect2F sporozoites (50%).

Recently, a study found that the sporozoite uses the sulfation level of heparan sulfate proteoglycans (HSPGs) on the surface of host cells as a Global Positioning System (Coppi et al., 2007). Sporozoites continue to migrate through cells expressing undersulfated HSPG and to switch to invasion in a PV into cells covered with highly sulfated HSPG, primarily hepatocytes. However, whether the cell surface sulfated signal acts to promote the formation of the MJ and PV or to silence cell traversal, or both, remains unknown. Theoretically, cessation of the cell traversal activity might be time dependent or induced upon contact with the target cell (possibly with HSPGs) or by cell traversal itself.

How cell traversal is achieved is also unclear. Sporozoites might directly rupture the host cell plasma membrane upon contact with the parasite, or initially enter inside the cell via a MJ and immediately escape from the vacuole. The former view would fit with the initial description of *P. berghei* sporozoites entering and exiting rodent peritoneal macrophages in a “needling manner and inducing an outward flow of host cell cytoplasm at the point of egress” (Vanderberg et al., 1990). The latter scenario would be reminiscent of the way sporozoites cross acinar cells of the mosquito salivary glands to reach the secretory cavities, i.e., by entering cells through the formation of a MJ while concomitantly lysing the membrane of the nascent PV (Pimenta et al., 1994).

In conclusion, the data presented here suggest that the host cell traversal activity ensures progression of the *Plasmodium* sporozoite from the site of mosquito bite to the liver parenchyma, where its repression allows final infection of a hepatocyte. One important function associated with the cell traversal activity is the resistance to killing by host phagocytic leukocytes, but

how this is achieved awaits further characterization. The picture that emerges from this and previous intravital imaging studies of the *Plasmodium* sporozoite in rodent hosts (Vanderberg and Frevort, 2004; Amino et al., 2006, 2007) is that the *Plasmodium* sporozoite relies on two robust abilities, host cell traversal and extracellular gliding, to reach its final niche in the liver. This contrasts with the strategy of the other well-studied and closely related Apicomplexan parasite, the *Toxoplasma* tachyzoite, which lacks cell traversal activity and hijacks host motile leukocytes for delivery to destination (Courret et al., 2006; Lambert et al., 2006).

EXPERIMENTAL PROCEDURES

Mosquitoes

Anopheles stephensi (Sda500 strain) mosquitoes were reared at the Centre for Production and Infection of *Anopheles* (CEPIA) at the Pasteur Institute using standard procedures. Mosquitoes were fed on infected mice 3–5 days after emergence and kept as already described (Amino et al., 2006, 2007). Infected mosquitoes used for transmission experiments (days 18–22 after the infectious blood meal) were deprived of sucrose for 1–2 days before experimentation to enhance the mosquito bite rate. For in vitro experiments, sporozoites were isolated from infected salivary glands 18–22 days after the infectious blood meal and kept on ice in tissue culture medium with 10% fetal calf serum (FCS).

Mice Manipulation

All experiments using rodents were approved by the committee of the Pasteur Institute and were performed in accordance with the applicable guidelines and regulations. For sporozoite analysis in lymph nodes, 10^4 salivary gland sporozoites in 3 μ l PBS were microinjected in the right (in the case of ConF sporozoites) and in the left (in the case of SpectF or Spect2F sporozoites) footpad. The popliteal lymph node was removed by minimally invasive surgery after 2 hr.

Microscopy and Image Analysis

Microscopic analysis was carried out using a high-speed spinning disk confocal system (Ultraview ERS, Perkin Elmer) mounted on an inverted Axiovert 200 microscope (Carl Zeiss) with Optovar option linked to a Orca II ER camera (Hamamatsu, Japan). Image files were processed using ImageJ. Sporozoites in the dermis of mice were imaged as already described (Amino et al., 2007).

Primary Hepatocytes

Rat (4-week-old female Wistar) and mouse (6- to 8-week-old female C57BL/6) hepatocytes (Janvier, France) were isolated from animals treated with sodium pentobarbital by a modified two-step collagenase perfusion method. Briefly, the liver was perfused via the portal vein for 10 min with liver perfusion medium 1 × (GIBCO 17701) followed by a 10 min perfusion with liver digest medium 1 × (GIBCO 17703) at a flow rate of 6–10 ml/min. Isolated cells were washed and centrifuged through a Percoll gradient to remove damaged cells. Cell viability (>90%) was determined by trypan blue exclusion. Hepatocytes were plated at a density of 6–15 × 10⁴ in 8-well permanox Lab-Tek chamber slides in Williams medium E containing 10% FCS. Cells were maintained at 37°C in a humidified atmosphere of 95% air and 5% CO₂.

Cell Traversal Assays

Cell traversal events by sporozoites were visualized by spinning disk confocal microscopy. Sporozoites and freshly trypsinized cells in a 1:1 ratio were mixed to 10 μl Matrigel (BD Biosciences) in the presence of 5 μM SYTOX Orange Nucleic Acid Stain (S-11368, Molecular Probes), a high-affinity nucleic acid stain that penetrates cells with a compromised plasma membrane. Samples were recorded for 30 min in multiple z layers with a double wavelength excitation of 488 nm and 568 nm for GFP-expressing parasites and SYTOX Orange, respectively.

Cell Infection Assays and CS Staining

Infection assays were performed at a multiplicity of infection of 1. Eight-well permanox Lab-Tek chamber slides and 15 × 10⁴ sporozoites freshly dissected out from mosquito salivary glands were used in experiments with rat primary hepatocytes; MatTek glass bottom culture dishes and 2 × 10⁴ sporozoites were used for CRL-2017 dermal fibroblasts infection. First, sporozoites were added onto cells on ice, and samples were centrifuged for 1 min at 4°C at 800 rpm to facilitate parasite-host cell interactions. Samples were then placed at 37°C, and at various incubation times samples were fixed with 4% paraformaldehyde (PFA), which does not permeabilize the host cell plasma membrane, and stained with the 3D11 anti-CS mAb coupled to Alexa Fluor 568 (A-20184, Molecular Probes). This allowed for discriminating between internalized sporozoites (green) and external sporozoites (red). Note that, in the case of the wild-type sporozoites, a proportion of the green parasites after 1 hr correspond to sporozoites that are located inside a cell, but not inside a vacuole (sporozoites arrested during cell traversal), a proportion that does not exceed 5%–10%.

Sporozoite Attachment Assay

Infection experiments were performed with 1.75 × 10⁴ salivary gland sporozoites and a confluent monolayer of CRL-2017 dermal fibroblasts plated on Lab-Tek chamber slides (8-well permanox). Sporozoites were plated on cells in the presence of cytD 1 μg/ml, and after 15 min at 37°C, samples were washed three times in PBS and then stained with an Ab-CS to differentiate intracellular from extracellular parasites. As expected, no intracellular parasites were found. In experiments with metabolic inhibited parasites, sporozoites were preincubated 1 hr at room temperature with 0.03% sodium azide and then plated on cells in the continued presence of this compound.

Transmission Electron Microscopy

Samples were fixed by addition of 2.5% glutaraldehyde/0.15 M cacodylate buffer followed by 1% osmium tetroxide, dehydrated in a series of ethanol concentrations, and embedded in EPON resin mixture. Ultrathin sections (50 to 60 nm) were observed with a Jeol 1200EXII (Tokyo, Japon) transmission electron microscope. Images were recorded using an Eloise Keenview camera and the Analysis Pro software version 3.1 (Eloise SARL, Roissy, France).

Real-Time Quantitative RT-PCR

Real-time qPCR was performed on cDNA preparations using the SYBR green detection system and the ABI Prism 7900 sequence detector (Applied Biosystems) according to the manufacturer's instructions. Salivary gland sporozoites from the ConF, SpectF, and Spect2F clones were isolated at day 21 after the blood meal. RNA was extracted with TriZol and DNase treated, and cDNAs synthesized with Superscript II reverse transcriptase (Invitrogen) using random primers. Three independent RNA preparations were made for each sample. PCR conditions were 1 cycle of 95°C for 10 min followed by 40 cycles of 95°C for 15 s, 55°C for 15 s, and 60°C for 45 min. qPCR was performed in triplicate with three serial dilutions. The standard curve was analyzed for all primers and gave amplification efficiencies of 90%–100%. Data were analyzed with SDS 2.1 software. Analysis was performed using the 2^{-ΔΔCt} method (User Bulletin 2, ABI). The following primers were used for qPCR analysis: Ama1, forward, ATTTGGGTTGATGGTTATTG; Ama1, reverse, TCCTTGTGCAAATTTGG TAG; CS, forward, ACAGAGGAATGGTCTCAATG; CS, reverse, TTATCCATT TACAAATTTCCAG; TRAP, forward, AACATTCCTCCATTCTTCC; TRAP, reverse, CATGTTATCCAATGCTCAC; P36p, forward, CTAATACGACCTTAG-GACACTTTGAA; P36p, reverse, GATGTTCCATTTGGGTTTACATGATC; P36, forward, GCCTAATGCAAAATATTATCCCGATTAG; P36, reverse, GCTAGT CCTTTGTTCCCATTTATATG; Pbp1/UIS10, forward, GTTACACTGATAGAGAA GATGT; Pbp1/UIS10, reverse, GTGGTACTATACAAACAATATGTTGG; Spect2, forward, AAGGAGTTTCAGCTATGCAC; Spect2, reverse, CAGTTCATTTATG CCTGACC; Spect1, forward, TAGCCTAATTCAAATAACGAAC; Spect1, reverse, GAAGTTAATTAATTCTGATACCCT; UIS4, forward, CCAAACCAAGCG ATCATACATACAG; UIS4, reverse, CTTACCCCACTAAATCGCTTAATTC; S6, forward, GCTAGTGAATCGAAGAAGC; S6, reverse, GCCTTGCAAATAATG AGAAC; Hsp70, forward, TGAGCAGATAATCAAACCT; Hsp70, reverse, ACTTCAATTTGTGGAACACC; PbActin, forward, GGAACATTATAACAGTA GGTAATGAAAG; PbActin, reverse, GTTGACTCCAGATAAAACAATGTTT CC; Tsrp, forward, TAAAGATAAGAGCACGAGTTAGTAGT; Tsrp, reverse, AATTGTTACATATTTACTTAGCATTCT; Celts, forward, GTTCTATGTTTGAG AGGCAAAAATGG; Celts, reverse, TGATGACGAGTCTTGTGAAATGCAC; UIS3, forward, AGTTGCAATTGCTTTGTTATCATCAGGA; UIS3, reverse, GTTCTTTATATTTGTACTAGTGTCTGGC.

Supplemental Data

The Supplemental Data include six supplemental figures and four supplemental movies and can be found with this article online at <http://www.cellhostandmicrobe.com/cgi/content/full/3/2/88/DC1/>.

ACKNOWLEDGMENTS

We thank S. Shorte, P. Roux, and the other members of the "Plateforme d'imagerie dynamique" (Institut Pasteur) for help with confocal microscopy; C. Bourguoin, I. Thiéry, and the other members of the "Centre de Production et d'Infection des Anophèles" (Institut Pasteur) for mosquito rearing; V. Richard from the Electron Microscopy Facility (University of Montpellier 2); G. Milon, G. Lauvau, and T. Graf for providing the *lys-gfp* mice; and Patricia Baldacci and Samantha Blazquez for comments on the manuscript. This work was supported by funds from the Institut Pasteur ("Grand Programme Horizontal Anopheles"), the Howard Hughes Medical Institute, the European Commission (FP6 BioMalPar Network of Excellence), and the Core Research for Evolutional Science and Technology (CREST). R.A. was supported by the Pasteur Institute GPH fellowship, D.G. is a BioMalPar Ph.D. student, T.I. was supported by a fellowship from the Association Pasteur-Japon, M.Y. is a CREST Scholar, and R.M. is a Howard Hughes Medical Institute International Scholar.

Received: August 2, 2007

Revised: October 18, 2007

Accepted: December 26, 2007

Published: February 13, 2008

REFERENCES

Amino, R., Martin, B., Thiberge, S., Celli, S., Shorte, S., Frischknecht, F., and Ménard, R. (2006). Quantitative imaging of *Plasmodium* transmission from mosquito to mammal. *Nat. Med.* 12, 220–224.

- Amino, R., Thiberge, S., Blazquez, S., Baldacci, P., Renaud, O., Shorte, S., and Ménard, R. (2007). Imaging malaria sporozoites in the dermis of the mammalian host. *Nat. Protocols* 2, 1705–1712.
- Baer, K., Roosevelt, M., Clarkson, A.B., Jr., van Rooijen, N., Schnieder, T., and Frevert, U. (2007). Kupffer cells are obligatory for *Plasmodium yoelii* sporozoite infection of the liver. *Cell. Microbiol.* 9, 397–412.
- Bhanot, P., Schauer, K., Coppens, I., and Nussenzweig, V. (2005). A surface phospholipase is involved in the migration of *Plasmodium* sporozoites through cells. *J. Biol. Chem.* 280, 6752–6760.
- Carrolo, M., Giordano, S., Cabrita-Santos, L., Corso, S., Vigarito, A.M., Silva, S., Leiriao, P., Carapau, D., Armas-Portela, R., Comoglio, P.M., et al. (2003). Hepatocyte growth factor and its receptor are required for malaria infection. *Nat. Med.* 9, 1363–1369.
- Coppi, A., Tewari, R., Bishop, J.R., Bennett, B.L., Lawrence, R., Esko, J.D., Billker, O., and Sinnis, P. (2007). Heparan sulfate proteoglycans provide a signal to *Plasmodium* sporozoites to stop migrating and productively invade host cells. *Cell Host Microbe* 2, 316–327.
- Courret, N., Darche, S., Sonigo, P., Milon, G., Buzoni-Gatel, D., and Tardieux, I. (2006). CD11c- and CD11b-expressing mouse leukocytes transport single *Toxoplasma gondii* tachyzoites to the brain. *Blood* 107, 309–316.
- Faust, N., Varas, F., Kelly, L.M., Heck, S., and Graf, T. (2000). Insertion of enhanced green fluorescent protein into the lysozyme gene creates mice with green fluorescent granulocytes and macrophages. *Blood* 96, 719–726.
- Frevert, U., Engelmann, S., Zougbede, S., Stange, J., Ng, B., Matuschewski, K., Liebes, L., and Yee, H. (2005). Intravital observation of *Plasmodium berghei* sporozoite infection of the liver. *PLoS Biol.* 3, e192. 10.1371/journal.pbio.0030192.
- Hollingdale, M.R., Leef, J.L., McCullough, M., and Beaudouin, R.L. (1981). *In vitro* cultivation of the exoerythrocytic stage of *Plasmodium berghei* from sporozoites. *Science* 213, 1021–1022.
- Ishino, T., Yano, K., Chinzei, Y., and Yuda, M. (2004). Cell-passage activity is required for the malarial parasite to cross the liver sinusoidal cell layer. *PLoS Biol.* 2, 77–84.
- Ishino, T., Chinzei, Y., and Yuda, M. (2005a). A *Plasmodium* sporozoite protein with a membrane attack complex domain is required for breaching the liver sinusoidal cell layer prior to hepatocyte infection. *Cell. Microbiol.* 7, 199–208.
- Ishino, T., Chinzei, Y., and Yuda, M. (2005b). Two proteins with 6-cys motifs are required for malarial parasites to commit to infection of the hepatocyte. *Mol. Microbiol.* 58, 1264–1275.
- Kaiser, K., Camargo, N., Coppens, I., Morrisey, J.M., Vaidya, A.B., and Kappe, S.H. (2004). A member of a conserved *Plasmodium* protein family with membrane-attack complex/perforin (MACPF)-like domains localizes to the micronemes of sporozoites. *Mol. Biochem. Parasitol.* 133, 15–26.
- Kappe, S.H., Buscaglia, C.A., and Nussenzweig, V. (2004). *Plasmodium* sporozoite molecular cell biology. *Annu. Rev. Cell Dev. Biol.* 20, 29–59.
- Kariu, T., Ishino, T., Yano, K., Chinzei, Y., and Yuda, M. (2006). CelTOS, a novel malarial protein that mediates transmission to mosquito and vertebrate hosts. *Mol. Microbiol.* 59, 1369–1379.
- Labaied, M., Camargo, N., and Kappe, S.H. (2007). Depletion of the *Plasmodium berghei* thrombospondin-related sporozoite protein reveals a role in host cell entry by sporozoites. *Mol. Biochem. Parasitol.* 153, 158–166.
- Lambert, H., Hitziger, N., Dellacasa, I., Svensson, M., and Barragan, A. (2006). Induction of dendritic cell migration upon *Toxoplasma gondii* infection potentiates parasite dissemination. *Cell. Microbiol.* 8, 1611–1623.
- Leiriao, P., Rodrigues, C.D., Albuquerque, S.S., and Mota, M.M. (2004). Survival of protozoan intracellular parasites in host cells. *EMBO Rep.* 5, 1142–1147.
- Matsuoka, H., Yoshida, S., Hirai, M., and Ishii, A. (2002). A rodent malaria, *Plasmodium berghei*, is experimentally transmitted to mice by merely probing of infective mosquito, *Anopheles stephensi*. *Parasitol. Int.* 51, 17–23.
- Ménard, R. (2001). Gliding motility and cell invasion by Apicomplexa: Insights from the *Plasmodium* sporozoite. *Cell. Microbiol.* 3, 63–73.
- Mota, M.M., Pradel, G., Vanderberg, J.P., Hafalla, J.C., Frevert, U., Nussenzweig, R.S., Nussenzweig, V., and Rodriguez, A. (2001). Migration of *Plasmodium* sporozoites through cells before infection. *Science* 291, 141–144.
- Mota, M.M., Hafalla, J.C.R., and Rodriguez, A. (2002). Migration through host cells activates *Plasmodium* sporozoites for infection. *Nat. Med.* 8, 1318–1322.
- Mota, M.M., and Rodriguez, A. (2004). Migration through host cells: The first steps of *Plasmodium* sporozoites in the mammalian host. *Cell. Microbiol.* 6, 1113–1118.
- Mueller, A.K., Camargo, N., Kaiser, K., Andorfer, C., Frevert, U., Matuschewski, K., and Kappe, S.H. (2005a). *Plasmodium* liver stage developmental arrest by depletion of a protein at the parasite-host interface. *Proc. Natl. Acad. Sci. USA* 102, 3022–3027.
- Mueller, A.K., Labaied, M., Kappe, S.H., and Matuschewski, K. (2005b). Genetically modified *Plasmodium* parasites as a protective experimental malaria vaccine. *Nature* 433, 164–167.
- Pimenta, P.F., Touray, M., and Miller, L. (1994). The journey of malaria sporozoites in the mosquito salivary gland. *J. Eukaryot. Microbiol.* 41, 608–624.
- Pradel, G., and Frevert, U. (2001). Malaria sporozoites actively enter and pass through rat Kupffer cells prior to hepatocyte invasion. *Hepatology* 33, 1154–1165.
- Prudencio, M., Rodriguez, A., and Mota, M.M. (2006). The silent path to thousands of merozoites: The *Plasmodium* liver stage. *Nat. Rev. Microbiol.* 11, 849–856.
- Sibley, L.D. (2004). Intracellular parasite invasion strategies. *Science* 304, 248–253.
- Sidjanski, S., and Vanderberg, J.P. (1997). Delayed migration of *Plasmodium* sporozoites from the mosquito bite site to the blood. *Am. J. Trop. Med. Hyg.* 57, 426–429.
- Silvie, O., Franetich, J.F., Charrin, S., Mueller, M.S., Siau, A., Bodescot, M., Rubinstein, E., Hannoun, L., Charoenvit, Y., Kocken, C.H., et al. (2004). A role for apical membrane antigen 1 during invasion of hepatocytes by *Plasmodium falciparum* sporozoites. *J. Biol. Chem.* 279, 9490–9496.
- Sinnis, P., Clavijo, P., Fenyó, D., Chait, B.T., Cerami, C., and Nussenzweig, V. (1994). Structural and functional properties of region II-plus of the malaria circumsporozoite protein. *J. Exp. Med.* 180, 297–306.
- Sturm, A., Amino, R., van de Sand, C., Regen, T., Retzlaff, S., Renneberg, A., Krueger, A., Pollok, J.M., Ménard, R., and Heussler, V.T. (2006). Manipulation of host hepatocytes by the malaria parasite for delivery into liver sinusoids. *Science* 313, 1287–1290.
- Sultan, A.A., Thathy, V., Frevert, U., Robson, K.J., Crisanti, A., Nussenzweig, V., Nussenzweig, R., and Ménard, R. (1997). TRAP is necessary for gliding motility and infectivity of *Plasmodium* sporozoites. *Cell* 90, 511–522.
- Vanderberg, J.P., Chew, S., and Stewart, M.J. (1990). *Plasmodium* sporozoite interactions with macrophages *in vitro*: A videomicroscopic analysis. *J. Protozool.* 37, 528–536.
- Vanderberg, J.P., and Frevert, U. (2004). Intravital microscopy demonstrating antibody-mediated immobilisation of *Plasmodium berghei* sporozoites injected into skin by mosquitoes. *Int. J. Parasitol.* 34, 991–996.
- van Dijk, M.R., Douradinha, B., Franke-Fayard, B., Heussler, V., van Dooren, M.W., van Schaijk, B., van Gemert, G.J., Sauerwein, R.W., Mota, M.M., Waters, A.P., and Janse, C.J. (2005). Genetically attenuated, P36p-deficient malarial sporozoites induce protective immunity and apoptosis of infected liver cells. *Proc. Natl. Acad. Sci. USA* 102, 12194–12199.
- van Rooijen, N., Bakker, J., and Sanders, A. (1997). Transient suppression of macrophage functions by liposome-encapsulated drugs. *Trends Biotechnol.* 15, 178–185.
- Waters, A.P., Mota, M.M., van Dijk, M.R., and Janse, C.J. (2005). Parasitology. Malaria vaccines: Back to the future? *Science* 307, 528–530.
- Yamauchi, L.M., Coppi, A., Snounou, G., and Sinnis, P. (2007). *Plasmodium* sporozoites trickle out of the injection site. *Cell. Microbiol.* 9, 1215–1222.